

Asian Journal of Chemistry; Vol. 28, No. 9 (2016), 1933-1943

ASIAN JOURNAL OF CHEMISTRY

<http://dx.doi.org/10.14233/ajchem.2016.19833>



Adsorption of Acid Blue 260 from Aqueous Solutions onto Multi-Wall Carbon Nanotube: Determination of Equilibrium, Thermodynamics Parameters by Linear and Non-linear Regression

M. SHABANI* and F. AZIZINEZHAD

Department of Chemistry, Islamic Azad University, Varamin-Pishva Branch, Varamin, Iran

*Corresponding author: Fax: +98 213 6725002; Tel: +98 213 6725011; E-mail: mshabani45@yahoo.com

Received: 11 January 2016;

Accepted: 17 April 2016;

Published online: 1 June 2016;

AJC-17920

This study examined the feasibility of removing acid blue 260, an acidic dye, from aqueous solutions using multi-wall carbon nanotube (MWCNTs). The dye adsorption experiments were carried out by using batch procedure. The effects of contact time, pH, dye concentration, adsorbent dose and temperature on adsorption of acid blue 260 by MWCNTs was also evaluated. This study used four two-parameter isotherms and six three-parameter isotherms. The equilibrium data were then analyzed using linear regression and one non-linear error analysis method. Experimental results have shown that the acidic pH (6.4), favoured the adsorption. The dye adsorption equilibrium was attained after 75 min of contact time. The capacity of MWCNTs to adsorb acid blue 260 was 233.34 mg/g in 298 K. The adsorption amount of acid blue 260, q_e (mg/g), increased as dye concentration and temperature increased. The equilibrium adsorption of acid blue 260 is best fitted in the linear regression Dubinin-Radushkevich isotherm at 298 K and non-linear regression Koble-Corigan model is best fitted at 308 and 318 K. For acid blue 260, enthalpy (ΔH°) and entropy (ΔS°) were 31.361 kJ/mol and 131.74 J/mol K, respectively.

Keywords: Adsorption, Acid blue 260, Multi-wall carbon nanotube, Isotherms, Thermodynamics.

INTRODUCTION

Dyes are one of the most hazardous chemical compounds classes found in industrial effluents including textile companies, dye manufacturers, food processing companies, paper and pulp mills and electroplating factories and need to be treated since their presence in water bodies reduces light penetration, precluding the photosynthesis of aqueous flora [1]. Additionally, some dyes are toxic to the environment. Most of the dyes contain aromatic rings, which make them carcinogenic and mutagenic [2,3]. Dyes can cause allergy, dermatitis and skin irritation [4]. Therefore, the removal of dyes from textile effluents is currently of great interest. Many treatment methods have been developed to remove dyes from wastewater. These treatment methods can be divided into physical, chemical and biological schemes. These include adsorption methods, coagulation processes, photo catalytic degradation and the ozone and hypochlorite treatment of dye waste effluents [5-7]. Although chemical and biological approaches are effective in removing dyes, they require special equipment and are usually energy intensive. These processes often generate large amounts of byproducts. Among all existing techniques, adsorption is considered the most efficient; additionally, adsorption is easily operated and insensitive to toxic substances. Physical adsorption, because of its low cost, high efficiency, easy handling,

wide variety of adsorbents and high stabilities toward the adsorbents, has become the most widely used method for eliminating dyes from wastewaters. Numerous adsorbents, such as activated carbons, zeolites, clays, industrial by-products, agricultural wastes, biomass and polymeric materials have been examined for their ability to remove some dyes from wastewater [8]. However, these adsorbents described above suffer from low adsorption capacities and separation inconvenience. Therefore, efforts are still needed to carry out investigation for new promising adsorbents. Carbon nanotubes (CNTs) as new adsorbents have gained increasing attention of many researchers [9-22]. According to the graphene layer, CNTs can be classified into single-wall carbon nanotubes (SWCNTs) and multi-wall carbon nano-tubes (MWCNTs) [23]. Carbon nanotubes are highly popular due to their novel properties like high aspect ratio, high thermal, electrical and mechanical properties [24-27]. High aspect ratio of CNTs makes them a possible candidate for water purification. Large surface area and high porosity provide enough adsorption sites for harmful cations, anions and other organic and inorganic impurities present in some natural sources of water. The outer surface of individual CNTs provides evenly distributed hydrophobic sites for organic chemicals.

This study explains the equilibrium and thermodynamics of adsorption of acid blue 260 by MWCNTs. Ten isotherm models were used for modeling the experimental equilibrium

data for acid blue 260 adsorption onto MWCNTs. The objectives of this study are to (i) determine the effects of dye concentration, pH, contact time and temperature on adsorption of acid blue 260 by MWCNTs, (ii) measure the coefficients of various two to three parameters isotherms and (iii) derive changes in thermodynamic parameters such as free energy (ΔG°), enthalpy (ΔH°) and entropy (ΔS°) during adsorption.

EXPERIMENTAL

Powders of MWCNTs, whose characteristics are indicated in Table-1, were purchased from Neutrino Corporation (Iran). Water-soluble, organic dye, acid blue 260 was provided by Institute for Color Science and Technology (Iran). Table-2 gives the molecular structure with other information regarding this dye.

Adsorption of acid blue 260 : Adsorption experiments were carried out by batch technique at room temperature (25 °C). Batch experiments included: contact time, pH, adsorption isotherms and temperature effects of adsorption. All of the acid blue 260 solution was prepared with distilled water. For all experiments, 10 mg MWCNTs was mixed with 25 mL acid blue 260 solution in a 100 mL Erlenmeyer flask and it was placed on a slow-moving platform shaker and the solution was shaken at 150 rpm for equilibrium time, 75 min. The effect of contact time on the amount of acid blue 260 adsorbed was investigated at 50 mg/L initial concentration of dye at 25 °C. The initial solution pH was fixed at pH 6.4, natural pH, (except when the effect of pH was studied). The pH of the solution was adjusted with 0.1 N HCl or 0.1 N NaOH solutions by using a Hanna Model HI83141 Digital pH-meter. The effect of pH on the used dye adsorption was determined over a range of pH from 3 to 10. To determine the point of zero charge of adsorbent (PZC), pH values of solutions of acid blue 260 were measured before and after of adsorption. Point of zero charge is the point that the initial and final pH is equal. At the end of the adsorption period, the solution was centrifuged for 10 min at 1,000 rpm. After centrifugation, the dye concentration in the supernatant solution was analyzed using a UV spectrophotometer (optima sp 3000+) by monitoring the absorbance changes at a wavelength of maximum absorbance (628 nm). The concentration of the dye was calculated using a standard curve based on the Lambert-Beer law. To determine the point

of zero charge of the MWCNTs, Milonjic *et al.* method [28] was used.

The amounts of dye adsorbed on MWCNTs were calculated from the concentrations in solutions before and after adsorption. At each experiment, the amount of acid blue 260 adsorbed (mg/g) (q_e), onto MWCNTs was calculated from the mass balance equation as follows:

$$q_e = \frac{V(C_0 - C_e)}{w}$$

where C_0 and C_e are the initial and equilibrium liquid-phase concentrations of acid blue 260 (mg/L), respectively; V = volume of acid blue 260 solution in liter and w = mass of MWCNTs sample used (g). Equilibrium isotherm studies were carried out with different initial concentration of acid blue 260 (10, 20, 30, 50, 75, 100 and 150 mg/L) at different temperatures (25, 35 and 45 °C).

RESULTS AND DISCUSSION

Characterization of the MWCNTs: Fig. 1(a) shows the SEM image for the MWCNTs. These nanotubes seemingly have a broad length distribution. The same MWCNTs appearance can be identified in the corresponding TEM image of Fig. 1(b).

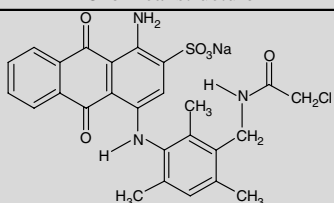
Raman spectra for MWCNTs are shown in Fig. 2. Two distinct bands found in the Raman spectrum of MWCNTs, which originate from different aspects of the nanotube, are the disordered mode (D mode) and the tangential mode (G band). The shape and intensity of the D mode at 1350 cm^{-1} correspond to the sp^3 hybridized carbon atoms, which is correlated with the extent of the nanotubes sidewall defects and the chemical sidewall functionalization. The higher frequency tangential G mode at 1590 cm^{-1} which is called the G' band is sensitive to the charge exchanged between the nanotubes and the guest moiety. The G band is thus an intrinsic feature of carbon nanotubes, which is closely related to vibrations in all sp^2 carbon materials [29]. The XRD patterns for the MWCNTs are shown in Fig. 3. The pattern of the MWCNTs shows a high intense peak at $2\theta = 25.2^\circ$ and a low intense peak at $2\theta = 44.0^\circ$, corresponding to the (002) and (100) reflections [30].

Effect of contact time: The influence of contact time on the adsorption capacity of MWCNTs is depicted in Fig. 4(a).

TABLE-1
SOME PROPERTIES OF MWCNTs

Purity	Outer diameter	Inner diameter	Length	Special surface area	Tap density	True density	Electric conductivity	Making method
> 95 %	< 8 nm	2-5 nm	> 10 μm	500 m^2/g	0.27 g/cm^3	2.1 g/cm^3	>100 s/cm	CVD

TABLE-2
CHEMICAL STRUCTURE AND SOME OTHER PARAMETERS OF THE ACID BLUE 260 DYE

Name	CAS number	m.f.	m.w.	λ_{max}	Chemical structure
Acid Blue 260	62168-86-9	$\text{C}_{26}\text{H}_{23}\text{N}_3\text{NaO}_6\text{SCl}$	563.99	628 nm	

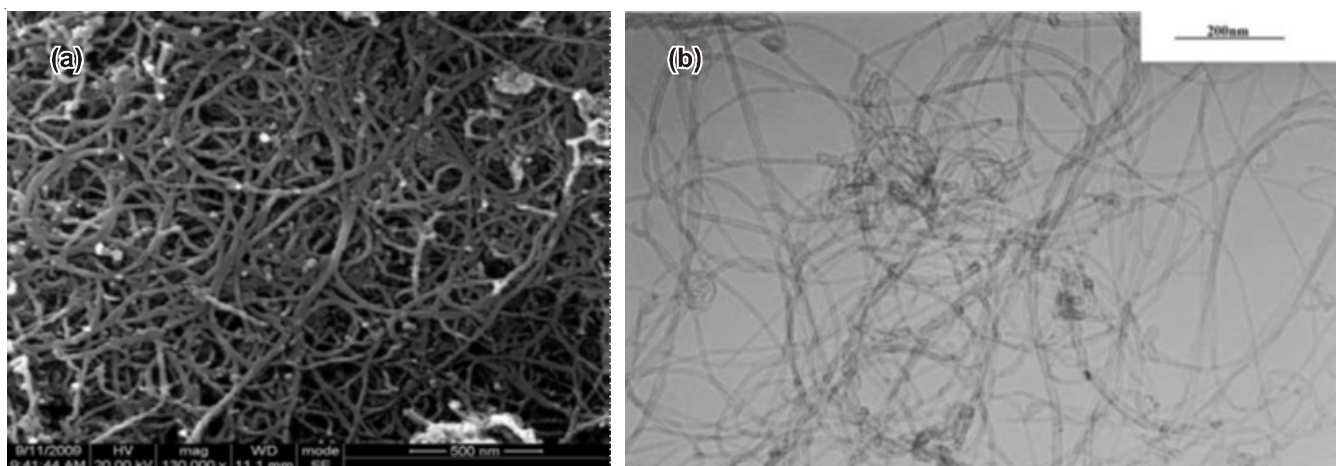


Fig. 1. (a) Scanning electron microscopy (SEM) and (b) transmission electron microscopy (TEM) of MWCNTs

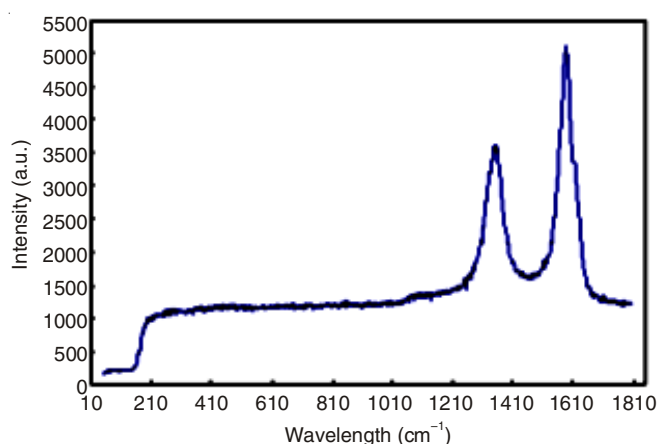


Fig. 2. Raman spectra of MWCNTs

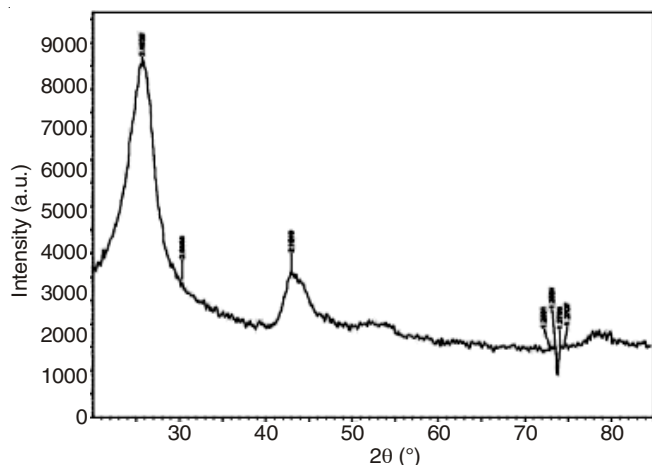


Fig. 3. X-ray diffraction of MWCNTs

It suggested that the amount of q_e reaches a constant number after 75 min (about 85 % adsorption of dye).

Effect of pH: The pH effect on the adsorption of acid blue 260 onto the MWCNTs was studied by evaluating the adsorption at pH values from 3 to 10 as shown in Fig. 4(b). It was found that maximum adsorption capacity of MWCNTs is occurred on its natural pH (6.4). As it is shown in Fig. 5(a), point of zero charge (PZC) of MWCNTs is 7. When MWCNTs is placed in aqueous solutions of pH below its PZC = 7 it

becomes protonated and exhibits a positive net charge on its surface. In contrast, when it placed in solutions above its PZC = 7, the net surface charge turns negative by deprotonation and it could adsorb the positively charged species. The results show that MWCNTs has the maximum efficiency to adsorb acid blue 260 when the adsorbent has no net charge on its surface.

Effect of temperature and initial concentration of dye:

The effect of temperature and initial concentration was studied with initial acid blue 260 concentrations ranging from 10 to 150 mg/L and 10 mg MWCNTs at 298-318 K. Fig. 5(b), shows the adsorption capacity *versus* initial acid blue 260 concentrations at 298, 308 and 318 K. It was clear that the adsorption of dye depends on the concentration of the dye. The adsorption capacity increased from 15.18 to 223.21 mg/g with the increase of dye concentration from 10 to 150 mg/L at 298 K. The initial dye concentration provides the necessary driving force to overcome the resistances to the mass transfer of acid blue 260 between the aqueous and solid phases. Temperature also has important effect on the adsorption process. The adsorption capacity of acid blue 260 onto MWCNTs was found to increase with increase in temperature. Maximum capacity of adsorbent experimentally found is 223.2, 255, 271.4 mg/g at 298, 308 and 318 K respectively. Fig. 5(b) shows that in high concentration of acid blue 260, multilayer adsorption occurred, especially at low temperatures.

Effect of MWCNTs dosage: The effect of the adsorbent dose was investigated by addition of various amounts of MWCNTs in 25 mL of 20 mg/L acid blue 260 aqueous solution at 298 K for 75 min. The result is shown in Fig. 6(a). It was observed that the removal efficiency increased from 44.9 to 87.2 % with an increase in adsorbent dose from 5 to 100 mg. This can be attributed to the increase in the adsorbent specific surface area and availability of more adsorption sites. Further increase in the amount of the adsorbent did not affect the removal efficiency significantly. It is also observed that the adsorption capacity decreases from 45 to 4.4 mg/g as the adsorbent dose increases from 5 to 100 mg. Consequently, the adsorbent dose was maintained at 10 mg in all the subsequent experiments, which was considered to be sufficient for the removal of acid blue 260.

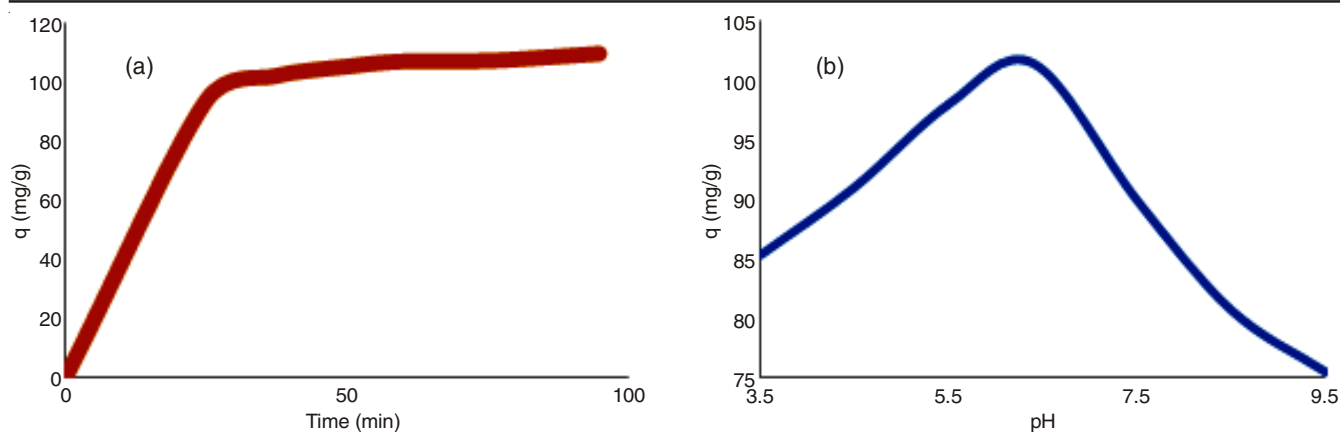


Fig. 4. (a) Effect of contact time on the amount of dye adsorbed on MWCNTs, (b) Effect of pH on the amount of acid blue 260 adsorbed on the MWCNTs, (Conditions: initial dye concentration = 50 ppm; Dosage of adsorbent = 10 mg; pH = 6.4; Agitation speed = 150 rpm)

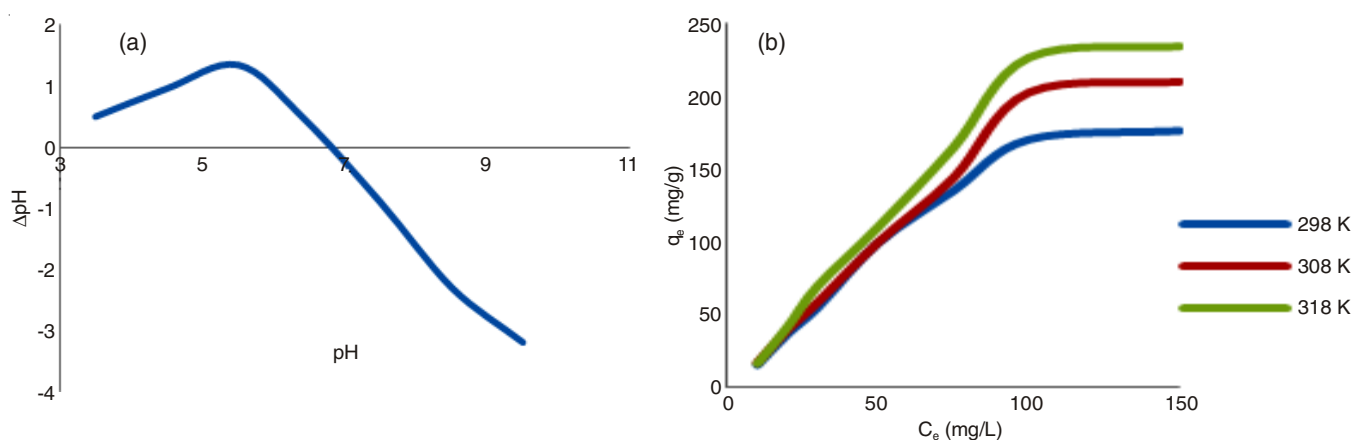


Fig. 5. (a) PZC determination of MWCNTs, (b) effect of temperature and initial concentration on adsorption of acid blue 260 onto MWCNTs

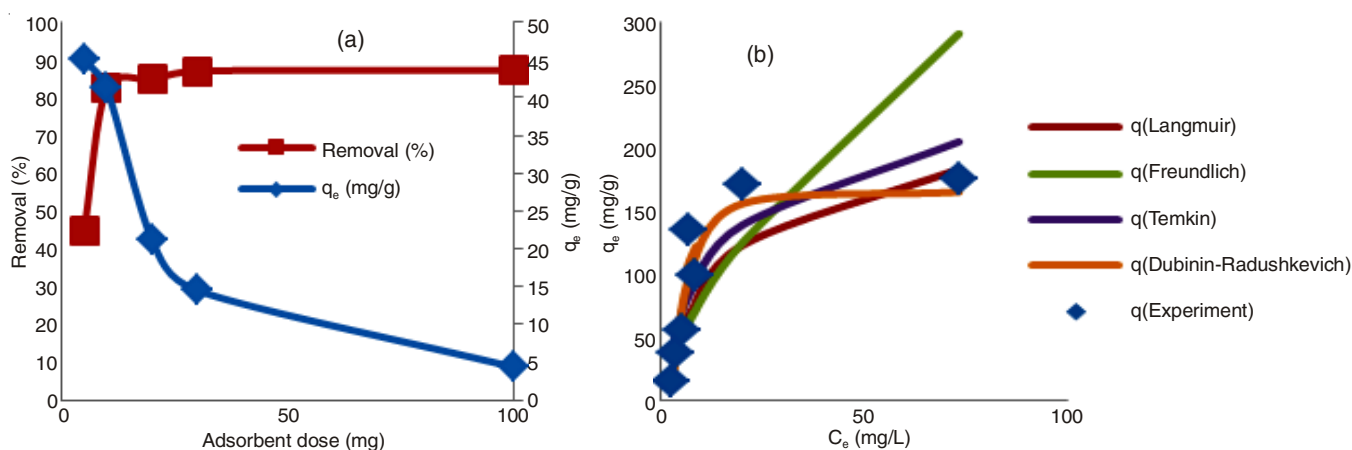


Fig. 6. (a) Effect of adsorbent dose on adsorption of acid blue 260 onto MWCNTs at 298 K. ($C_0 = 20$ mg/L), (b) Linear two-parameter isotherms models for the adsorption of acid blue 260 onto MWCNTs at 298 K

Adsorption isotherms: The quantity of dye that could be taken up by MWCNTs is a function of both the concentration of the dye and the temperature. The amount of material adsorbed is determined as a function of the concentration at a constant temperature that could be explained in adsorption isotherms. The adsorption isotherms show how solute interacts with the sorbent.

Experimental results have been analyzed using four two-parameter isotherm models Langmuir, Freundlich, Temkin and Dubinin-Radushkevich, six three-parameter adsorption isotherm models Redlich Peterson, Sips, Toth, Khan, Koble-Corrigan and Radke-Prausnitz. Table-3 shows non-linear and linear form (if exists) of isotherms. Sum of the squares of error (SSE) analysis method was used to determine the isotherm parameters. R^2

TABLE-3 LISTS OF ADSORPTION ISOTHERM MODELS		
Isotherm	Non-linear form	Linear form
Two parameters		
Langmuir	$q_e = \frac{q_m K_a C_e}{1 + K_a C_e}$	$\frac{C_e}{q_e} = \frac{1}{q_m} C_e + \frac{1}{K_a q_m}$
Freundlich	$q_e = K_F C_e^{1/n}$	$\ln(q_e) = \ln(K_F) + \frac{1}{n} \ln(C_e)$
Temkin	$q_e = B_T \ln A_T + B_T \ln(C_e)$	$q_e = \left(\frac{RT}{b_T}\right) \ln A_T + \left(\frac{RT}{b_T}\right) \ln(C_e)$
Dubinin-Radushkevich	$q_e = q_0 \exp(-K_{ad} \epsilon^2)$	$\ln(q_e) = \ln(q_0) - K_{ad} \epsilon^2$
Three parameters		
Redlich-Peterson	$q_e = \frac{K_R C_e}{1 + a_R C_e^g}$	$\ln\left(K_R \frac{C_e}{q_e} - 1\right) = g \ln(C_e) + \ln(a_R)$
Sips	$q_e = \frac{K_s a_s C_e^B}{1 + a_s C_e^B}$	$\ln\left(\frac{K_s}{q_e} - 1\right) = -B_s \ln(C_e) - \ln(a_s)$
Toth	$q_e = \frac{q_m a_T C_e}{(1 + (a_T C_e)^t)^{1/t}}$	
Khan	$q_e = \frac{q_s b_k C_e}{(1 + b_k C_e)^{a_k}}$	
Koble-Corrigan	$q_e = \frac{a C_e^n}{1 + B C_e^n}$	$\frac{1}{q_e} = \frac{1}{A} \frac{1}{C_e^n} + \frac{B}{A}$
Radke-Prausnitz	$q_e = \frac{a_{RP} C_e}{1 + \left(\frac{a_{RP}}{r_R}\right) C_e^{\beta_k}}$	

values were used to find the best model. The calculations were made using the solver of excel 03 software.

Two parameter models

Langmuir model: The Langmuir model assumes that there is no interaction between the adsorbate molecules and the adsorption is localized in a monolayer [31]. K_a is a coefficient related to the affinity between the sorbent and sorbate. The linear and non-linear form of Langmuir isotherm is indicated in Table-3. The linear and non-linear regression of four two-parameter isotherms plots 298, 308 and 318 K are presented in Figs. 6-9, respectively. Numerical results for linear and non-linear regression for two-parameter isotherms are given in Table-4. The results show that the linear regression is not good

for these data, because the square of correlation coefficient is too far from 1, but the predicted q_m for 298K is nearly equals to experiment.

The experimental data have good agreement with Langmuir isotherm model when we use non-linear regression. The K_a constant increases with increasing the temperature.

Langmuir isotherm determines whether the adsorption is favourable or unfavourable. To determine the characteristic behaviour of the adsorption, a dimensionless constant, commonly known as separation factor (R_L) defined by Webber and Chakkravorti [32] can be represented as:

$$R_L = \frac{1}{1 + K_a C_0} \tag{1}$$

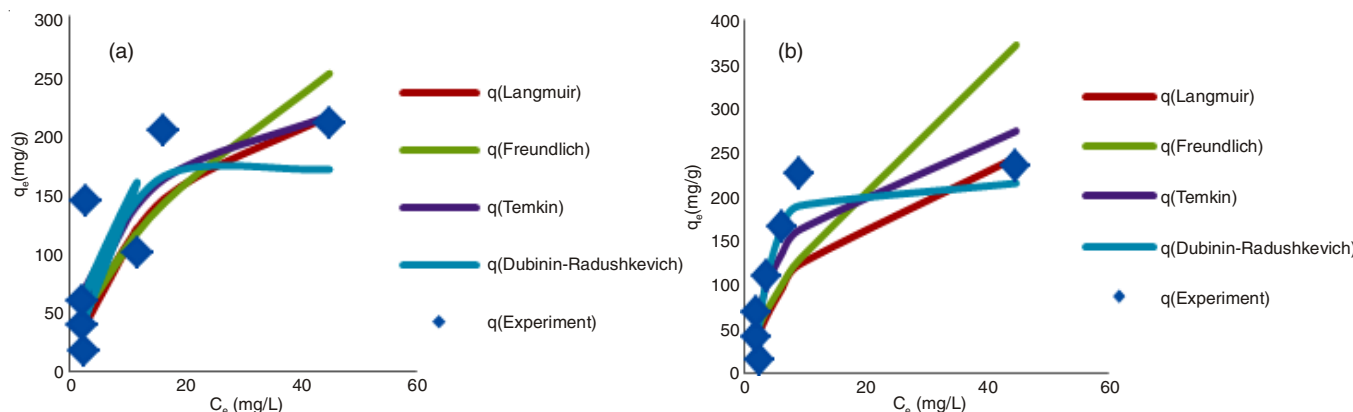


Fig. 7. Linear two-parameter isotherms models for the adsorption of acid blue 260 onto MWCNTs at (a) 308K and (b) 318 K

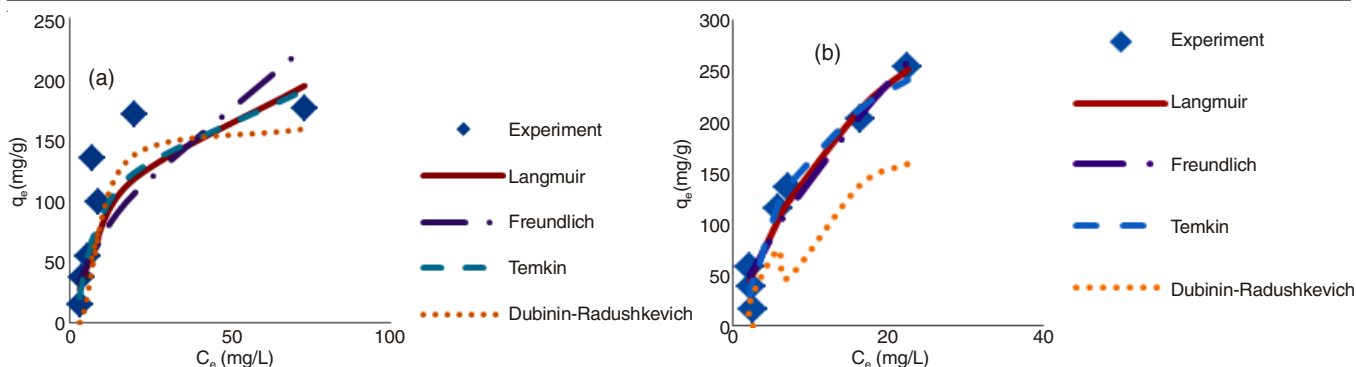


Fig. 8. Non-linear two-parameter isotherms models for the adsorption of acid blue 260 onto MWCNTs at (a) 298 K and (b) 308 K

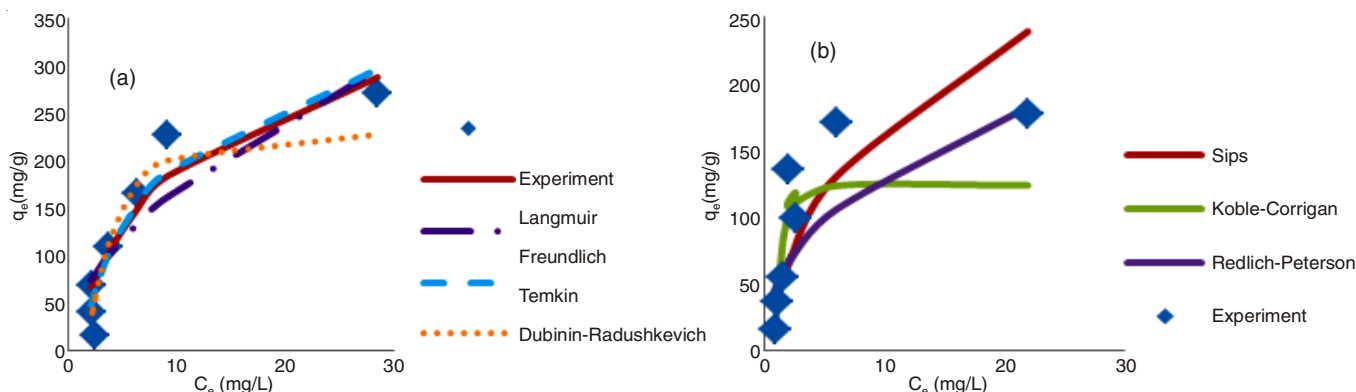


Fig. 9. (a) Non-linear two-parameter isotherms models at 318 K and (b) Linear three-parameter isotherms models at 298K for the adsorption of acid blue 260 onto MWCNTs

where, C_0 = highest initial dye concentration. For a favourable adsorption R_L value must be between 0 and 1. While $R_L > 1$, $R_L = 1$ and $R_L = 0$ indicate unfavourable, linear and irreversible adsorption processes respectively. The R_L values were found to be between 0.19 to 0.67 for different temperatures which shows favourable adsorption onto the adsorbent.

Freundlich model: Freundlich isotherm is an isotherm describing the non-ideal and reversible adsorption, not restricted to the formation of monolayer. This empirical model can be applied to multilayer adsorption, with non-uniform distribution of adsorption heat and affinities over the heterogeneous surface [33]. The slope ($1/n$) ranges between 0 and 1 is a measure of adsorption intensity or surface heterogeneity, becoming more

heterogeneous as its value gets closer to zero. Whereas, a value below unity implies chemisorptions process where ($1/n$) above one is an indicative of cooperative adsorption [34]. The linear regression of Freundlich isotherm plot for the adsorption of acid blue 260 onto MWCNTs in three different temperatures are shown in Figs. 6 and 7. Non-linear regression results are shown in Figs. 8 and 9. The value of n (Table-4) for this adsorption were determined is between 1.11 to 1.41 for linear method and 1.4 to 1.88 for non-linear method. It indicated that this adsorption is favourable.

Temkin model: Temkin isotherm [35] contains a factor that explicitly taking into the account of adsorbent-adsorbate interactions. This model assumes that heat of adsorption of all

TABLE-4
RESULTS OF REGRESSION OF TWO-PARAMETER ISOTHERMS FOR ADSORPTION OF ACID BLUE 260 ONTO MWCNT

Temp. (K)	Para-meters	Langmuir		Para-meters	Freundlich		Para-meters	Temkin		Para-meters	Dubinin-Radushkevich	
		Linear	Non-linear		Linear	Non-linear		Linear	Non-linear		Linear	Non-linear
298	q_m	266.763	257.227	K_f	13.6984	18.6405	A_T	0.20929	0.20929	q_0	138.043	161.208
	K_a	0.03483	0.04267	n	1.48157	1.71896	B_T	52.3858	52.3858	K_{ad}	3.88499	10.5
	R^2	0.62305	0.83668	R^2	0.81902	0.85379	R^2	0.81718	0.84544	R^2	0.91858	0.75886
	R_L	0.16064	0.13512							E	0.35875	0.21815
308	q_m	1793.81	498.006	K_f	17.6884	28.1365	A_T	0.10087	0.10087	q_0	188.483	180.0
	K_a	0.00803	0.04551	n	1.11063	1.40183	B_T	90.2822	90.2822	K_{ad}	1.97883	2.11
	R^2	0.01328	0.96128	R^2	0.78348	0.95805	R^2	0.96032	0.96183	R^2	0.71492	0.83940
	R_L	0.45373	0.65745							E	0.50267	0.48695
318	q_m	707.259	394.446	K_f	23.7749	50.1098	A_T	0.01680	0.01680	q_0	229.039	230
	K_a	0.02643	0.09606	n	1.18159	1.88124	B_T	95.8023	95.8023	K_{ad}	1.830	1.80
	R^2	0.08288	0.89345	R^2	0.64541	0.83119	R^2	0.90825	0.91596	R^2	0.67423	0.91164
	R_L	0.20145	0.26808							E	0.52265	0.52731

molecules in the layer would decrease linearly with coverage. The linear regression of Temkin isotherm plot for the adsorption of acid blue 260 onto MWCNTs in three different temperatures are shown in Figs. 6 and 7. Non-linear regression results are shown in Figs. 8 and 9. The results show that binding energy (B_T) increases with increasing temperature.

Dubinin-Radushkevich model: Dubinin-Radushkevich isotherm [36] is an empirical model initially conceived for the adsorption of subcritical vapours onto micropore solids following a pore filling mechanism. It is generally applied to express the adsorption mechanism with a Gaussian energy distribution onto a heterogeneous surface. The approach was usually applied to distinguish the physical and chemical adsorption of metal ions, with its mean free energy, E per molecule of adsorbate (for removing a molecule from its location in the sorption space to the infinity) can be computed by the relationship:

$$E = \frac{1}{\sqrt{2K_{ad}}} \quad (2)$$

where, K_{ad} is denoted as the isotherm constant. Meanwhile, the parameter ϵ can be correlated as:

$$\epsilon = RT \ln \left(1 + \frac{1}{C_e} \right) \quad (3)$$

where, R , T and C_e represent the gas constant (8.314 J/mol K), absolute temperature (K) and adsorbate equilibrium concentration (mg/L), respectively. The linear regression of Dubinin-Radushkevich isotherm plot for the adsorption of acid blue 260 onto MWCNTs in three different temperatures are shown in Figs. 6 and 7. Non-linear regression results are shown in Figs. 8 to 9. The results show that the mean free energies for acid blue 260 sorption process in three different temperatures are 0.21 to 0.52 kJ/mol. It indicates that the sorption process is physisorption. With increasing temperature, the mean energy value increases. It means that the tendency of acid blue 260 to adsorb onto MWCNTs increases with increasing temperature. Theoretical isotherm saturation capacity (q_s) in three different temperatures is far less than their experimental values, but q_s increases with increasing temperature.

Finally, for four two-parameter isotherms mentioned above, linear regression of Dubinin-Radushkevich isotherm is best

fitted in 298 K. For 308 and 318 K, non-linear regression of Temkin isotherm has best R^2 .

Three parameter models

Redlich-Peterson model: Redlich-Peterson isotherm [37] is a hybrid isotherm featuring both Langmuir and Freundlich isotherms, which incorporate three parameters into an empirical equation. The model represents adsorption equilibria over a wide concentration range, that can be applied either in homogeneous or heterogeneous systems due to its versatility. Typically, a minimization procedure is adopted in solving the equations by maximizing the correlation coefficient between the experimental data points and theoretical model predictions with solver add-in function of the Microsoft excel. In the limit, it approaches Freundlich isotherm model at high concentration (as the exponent g tends to zero) and is in accordance with the low concentration limit of the ideal Langmuir condition (as the all g values are close to one). The linear regression of Redlich-Peterson isotherm plot for the adsorption of acid blue 260 onto MWCNTs in three different temperatures are shown in Figs. 9 and 10. The non-linear regression of six three-parameter isotherms plots in 298, 308 and 318 K are presented in Figs. 11 and 12, respectively. Numerical results for linear and non-linear regression for three-parameter isotherms are given in Table-5. The results show that the linear regression is not good for these data. Instead, non-linear results have good agreement with experimental results. With increasing the temperature, the exponent g values become closer to unity. So, Langmuir behaviour preferred at high temperatures.

Sips model: Sips isotherm [38] is a combined form of Langmuir and Freundlich expressions deduced for predicting the heterogeneous adsorption systems and circumventing the limitation of the rising adsorbate concentration associated with Freundlich isotherm model. At low adsorbate concentrations, it reduces to Freundlich isotherm; while at high concentrations, it predicts a monolayer adsorption capacity characteristic of the Langmuir isotherm. The B_s parameter is usually greater than unity. The greater value of B_s indicates that system is more heterogeneous. The linear regression of Sips isotherm plot for the adsorption of acid blue 260 onto MWCNTs in three different temperatures are shown in Figs. 9 and 10. Non-linear regression results are shown in Figs. 11 and 12. The isotherm parameters are indicated in Table-5. As it is shown, the predicted

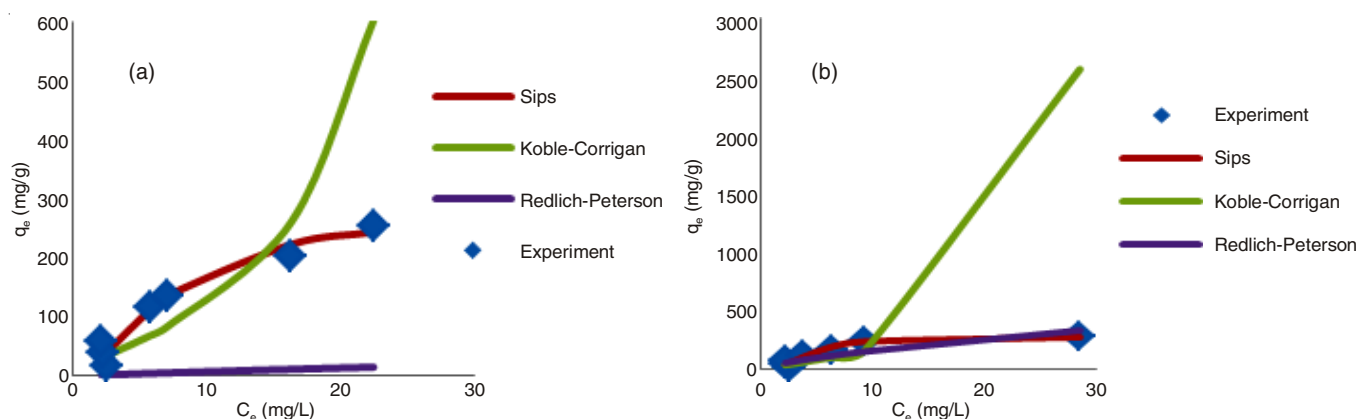


Fig. 10. Linear three-parameter isotherms models for the adsorption of acid blue 260 onto MWCNTs at (a) 308 K and (b) 318 K

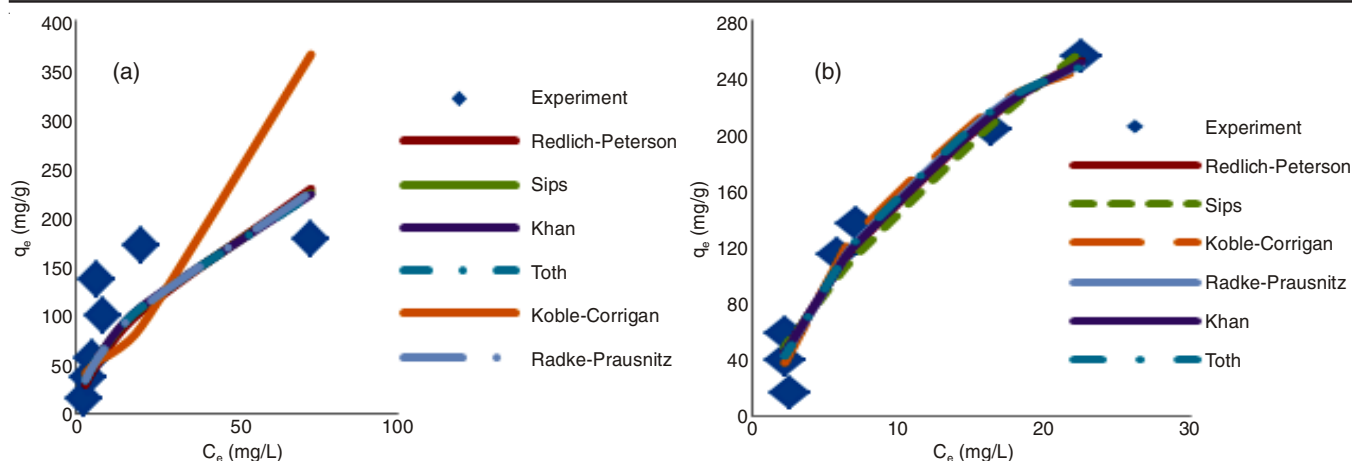


Fig. 11. Non-linear three-parameter isotherms models for the adsorption of acid blue 260 onto MWCNTs at (a) 298 K and (b) 308 K

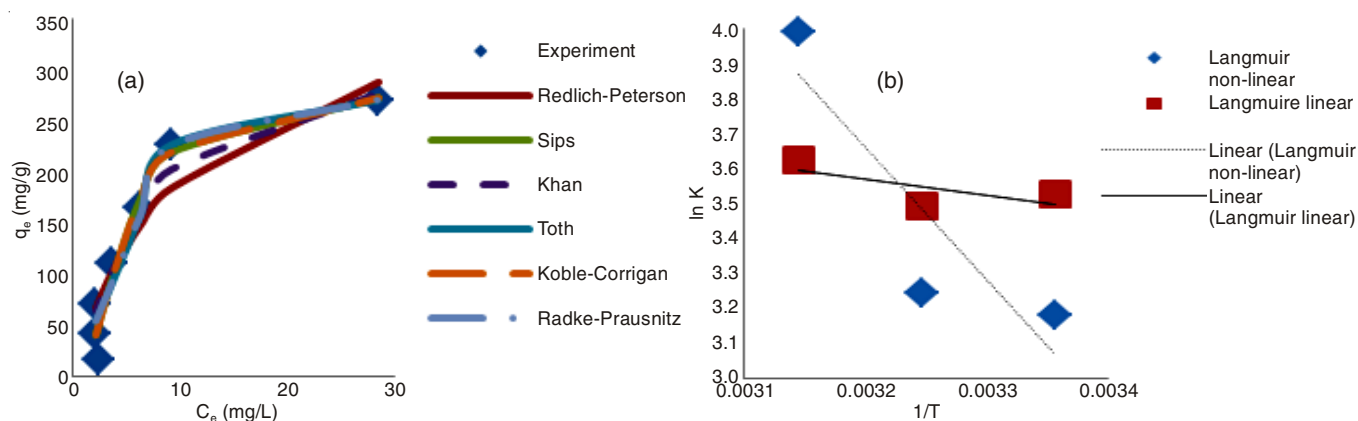


Fig. 12. Non-linear three-parameter isotherms models for the adsorption of acid blue 260 onto MWCNTs at (a) 318 K and (b)

TABLE-5
RESULTS OF REGRESSION OF THREE-PARAMETER ISOTHERMS FOR ADSORPTION OF ACID BLUE 260 DYE ONTO MWCNTs

Temp.	Parameters	Redlich-Peterson		Sips		Koble-Corrigan		Khan		Toth		Radke-Prausnit			
		L	NL	L	NL	L	NL	NL	NL	NL	NL				
298	K_R	260	41.344	K_S	432.599	5899.558	A	0.178	1.150	q_S	19.828	q_m	1387.97	a_{RP}	438.642
	a_R	8.2307	1.9447	a_S	0.0275	0.00314	B	0.00160	-0.964	b_K	1.123	a_T	0.0135	r_R	19.226
	g	0.5891	0.4277	B_S	0.842	0.591	n	4.423	0.00789	a_K	0.449	t	0.376	β_k	0.424
	R^2	0.3229	0.8509	R^2	0.8398	0.8534	R^2	0.9764	0.8708	R^2	0.8541	R^2	0.8491	R^2	0.8538
308	K_R	26.6	22.666	K_S	280.030	5619.884	A	14.894	14.663	q_S	683.050	q_m	322.986	a_{RP}	20.655
	a_R	6.78	0.0455	a_S	0.0330	0.00495	B	-0.127	0.0458	b_K	0.0328	a_T	0.0618	r_R	1468.66
	g	0.119	1	B_S	1.713	0.683	n	0.606	1.373	a_K	1.264	t	1.707	β_k	1.323
	R^2	0.1921	0.9613	R^2	0.8994	0.9511	R^2	0.4615	0.9660	R^2	0.9649	R^2	0.9629	R^2	0.9623
318	K_R	112.95	37.889	K_S	273.1	279.97305	A	15.263	9.636	q_S	33659.347	q_m	271.354	a_{RP}	25.437
	a_R	2.893	0.0961	a_S	0.0186	0.0344	B	-0.0494	0.0344	b_K	0.000977	a_T	0.0928	r_R	2211827
	g	0.3314	1	B_S	2.611	2.106	n	0.864	2.106	a_K	44.337	t	10.381	β_k	3.550
	R^2	0.0628	0.8934	R^2	0.935	0.9568	R^2	0.3552	0.9568	R^2	0.9252	R^2	0.9503	R^2	0.9500

L = Linear, NL = Non-linear

K_S value by linear and non-linear regression in 298 and 308 K are too different from each others, but this value in 318 K is nearly same in these two methods of regression. The B_S values increases with increasing the temperature.

Toth model: Toth [39] has modified the Langmuir equation to reduce the error between experimental data and predicted values of equilibrium adsorption data. This model is useful in describing heterogeneous adsorption systems, which satisfying

both low and high-end boundary of the concentration. Its correlation presupposes an asymmetrical quasi-Gaussian energy distribution. The most of its sites has adsorption energy lower than the maximum or mean value [24,40]. The exponent, $1/t$ lies between 0 and 1. When $t = 1$, the Toth isotherm reduces to the famous Langmuir equation; hence parameter t is said to characterize the system heterogeneity. Non-linear regression results are shown in Figs. 10 to 11 and the isotherm parameters are

indicated in Table-5. With increasing temperature the t value increases. It indicates that the heterogeneity of surfaces increases with increasing temperature.

Khan model: Khan isotherm [41] is a generalized model suggested for the pure solutions, which can represent both Langmuir and Freundlich type. The non-linear regression results are shown in Figs. 10 to 11 and the isotherm parameters are indicated in Table-5. The theoretical isotherm saturation capacity (q_s) values that predicted from squares of the errors minimization vary from 36.7 to 33659 at 298 to 318 K.

Koble-Corrigan model: Koble-Corrigan isotherm [42] incorporated both Langmuir and Freundlich isotherm models for representing the equilibrium adsorption data. The isotherm constants, A , B and n are evaluated from the linear plot using a trial and error optimization. The linear regression of Koble-Corrigan isotherm plot for the adsorption of acid blue 260 onto MWCNTs in three different temperatures are shown in Figs. 9 and 10. The non-linear regression results are shown in Figs. 11 to 12 and the isotherm parameters are indicated in Table-5. The linear regression results are not so good and R^2 values are so far from 1 for 308 and 318 K and predicted isotherm parameters are not reasonable, but the non-linear regression results provide the best fit with the experimental data in comparison with the other three parameters isotherm models.

Radke-Prausnitz model: Radke-Prausnitz model [43] is another three parameter isotherm which was obtained by a slight modification on the Langmuir equation. The non-linear regression results are shown in Figs. 11 to 12 and the isotherm parameters are indicated in Table-5. The results show that this model has a good agreement with experiment data.

Finally, for six three-parameter isotherms mentioned above, non-linear regression of Koble-Corrigan isotherm is best fitted at 298, 308 and 318 K.

Error functions: For non-linear regression studies of isotherms, the optimization procedure requires an error function to be defined in order to be able to evaluate the fit of the isotherm to the experimental equilibrium data. In this study, the sum of the squares of the errors (SSE) was examined and the isotherm parameters were determined by minimizing this error function across the concentration range studied [44]. The coefficient of determination (R^2), was used to compare which isotherms have the best fit experimental data. The error functions studied were as follows.

The sum of the squares of the errors method can be represented by the eqn. 4.

$$\sum_{i=1}^n (q_{\text{exp}} - q_{\text{cal}})_i^2 \quad (4)$$

where n is number of data point. The squares of the errors error function is the most common error function in use.

Coefficient of determination (R^2): R^2 is a statistic that will give some information about the goodness of fit of a model.

In regression, the R^2 coefficient of determination is a statistical measure of how well the regression results approximate the real data points. A R^2 of 1 indicates that the regression line perfectly fits the data. The R^2 formula is shown in eqn. 5.

$$R^2 = \frac{\sum_{i=1}^n (q_{\text{exp}} - \bar{q}_{\text{cal}})^2}{\sum_{i=1}^n (q_{\text{exp}} - \bar{q}_{\text{cal}})^2 + \sum_{i=1}^n (q_{\text{exp}} - q_{\text{cal}})^2} \quad (5)$$

where \bar{q}_{cal} = average of q_{cal} . In this study, the R^2 value was calculated for each regression to determine the goodness of fit of isotherms models.

Thermodynamic analyses: To estimate the effect of temperature on the adsorption of acid blue 260 onto MWCNTs, the free energy change (ΔG°), enthalpy change (ΔH°) and entropy change (ΔS°) were determined. The Langmuir isotherm was used to calculate thermodynamic parameters using the following equations:

$$\Delta G^\circ = -RT \ln K_a \quad (6)$$

$$\ln K_a = \frac{\Delta S^\circ}{R} - \frac{\Delta H^\circ}{R T} \quad (7)$$

where K_a = Langmuir equilibrium constant (L/mol). Considering the relationship between ΔG° and K_a , ΔH° and ΔS° were determined from the slope and intercept of the van't Hoff plots of $\ln(K_a)$ versus $1/T$. Table-6 presents the thermodynamic parameters at various temperatures. The values of K_a determined by linear and non-linear regression methods. The values of ΔG° in linear and non-linear method are negative. These values of ΔG° confirm the feasibility of the process and the spontaneous nature of the adsorption. In linear method, the values of ΔG° increase from -7.378 to -7.143 kJ/mol using the equilibrium constant (K_a) in contrast, in non-linear method, the values of ΔG° decrease. The decrease in the negative value of ΔG° with an increase in temperature indicates that the adsorption process of acid blue 260 on MWCNTs becomes more favourable at higher temperatures. It should be mentioned that the maximum capacity of adsorbent increases by increasing the temperature from 223.2 to 271.4 mg/g. So, the results of non-linear method are reasonable and the thermodynamic parameters obtained by non-linear method were considered. The values of ΔH° and ΔS° calculated from the plot of $\ln(K_a)$ versus $1/T$ [Fig. 12(b)]. The values of ΔH° and ΔS° are 31.361 kJ/mol and 131.74 J/mol K, respectively. The value of ΔH° is less than 40 kJ/mol, so based on Kara *et al.* [45], the adsorption of acid blue 260 onto MWCNTs is a physisorption process. The value of ΔH° is positive, indicating that the adsorption reaction was endothermic. The positive value of ΔS° reflects the affinity of MWCNTs for acid blue 260 and suggests some structural changes in dye and MWCNTs.

TABLE-6
VALUES OF THERMODYNAMIC PARAMETERS FOR THE ADSORPTION OF ACID BLUE 260 ONTO MWCNTs

Temp. (K)	ΔG° (kJ/mol)		ΔH° (kJ/mol)		ΔS° (J K ⁻¹ mol ⁻¹)		R^2	
	Linear	Non-linear	Linear	Non-linear	Linear	Non-linear	Linear	Non-linear
298	-7.378	-7.881						
308	-3.867	-8.310	-12.011	31.361	-19.1	131.74	0.038	0.7942
318	-7.143	-10.555						

Conclusions

In this study, the effects of parameters such as contact time, pH, dye concentration, adsorbent dose, isotherm studies, error analysis and temperature on adsorption of acid blue 260 by MWCNTs has been investigated. Ten isotherm equations containing two and three parameters were used to analysis equilibrium adsorption data. The equilibrium data were then analyzed using linear regression and non-linear error analysis method. The optimum pH was determined to be 6.4. The results showed adsorption increased as contact time increased and maximum percentage of removal was observed at 75 min. Isotherm studies showed that non-linear regression in the most of the isotherms have better R^2 than linear regression. It is important to choose the reasonable initial parameters for non-linear regression to reach the global minimum. Based on R^2 values, linear regression of Dubinin-Radushkevich and non-linear regression of Freundlich at 298 K have good agreement with experimental data for two parameters isotherm models. While, at 308 K non-linear Temkin and Langmuir models at 318 K non-linear Temkin and Dubinin-Radushkevich models have better agreement with experimental data.

Koble-Corrigan and Khon models at 298 and 308 K and Koble-Corrigan and Sip models at 318 K seem to provide the best fit with the experimental data compared the other three parameter isotherm models. The R^2 values in six three parameters models are very close to each others. So all of these isotherm have good agreement fit with experimental data. In comparison of all isotherms, the linear regression Dubinin-Radushkevich isotherm at 298 K and non-linear regression Koble-Corrigan model is best fitted at 308K and 318K. Based on average values of R^2 , three and two parameters isotherm models have good agreement with experimental data subsequently.

For acid blue 260, enthalpy (ΔH°) and entropy (ΔS°) were 31.361 kJ/mol and 131.74 J/mol K, respectively. The values of ΔG° in linear and non-linear method are negative. The values of ΔG° decrease with increasing temperature. It indicates that the adsorption process of acid blue 260 on MWCNTs becomes more favourable at higher temperatures. Finally, the results of this study indicate that the MWCNTs have good potential for adsorbing acid blue 260 from aqueous solutions.

Nomenclature

A	Koble-Corrigan isotherm constant $\text{mg}^{(1-n)}\text{L}^{-n}\text{g}^{-1}$
a_K	Khan isotherm model exponent
a_{PR}	Radke–Prausnitz isotherm model constant (L/g)
a_R	Redlich-Peterson isotherm constant (L/mg) ^{-S}
a_S	Sips isotherm model constant (L/mg) ^{-B_S}
A_T	Temkin isotherm constant (L/mg)
a_T	Toth isotherm constant (L/mg)
B	Koble-Corrigan isotherm constant (L/mg) ⁻ⁿ
b_K	Khan isotherm model constant (L/mg)
B_S	Sips isotherm model exponent
B_T	Temkin isotherm constant, related to the heat of adsorption (J/mol)
C_e	Equilibrium concentration of adsorbate (mg/L)
E	Mean free energy (kJ/mol)
G	Redlich-Peterson isotherm exponent

K_a	Langmuir isotherm constant (L/mg)
K_{ad}	Dubinin–Radushkevich isotherm constant (mol^2/kJ^2)
K_f	Freundlich isotherm constant ($\text{mg}^{(1-n)}\text{L}^n\text{g}^{-1}$)
K_R	Redlich-Peterson isotherm constant (L/g)
K_S	Sips isotherm model constant (mg/g)
n	Freundlich isotherm constant related to adsorption Intensity
q_0	Dubinin-radushkevich maximum adsorption capacity (mg/g)
q_{cal}	Theoretical equilibrium capacity (mg/g)
q_e	Equilibrium adsorption capacity of adsorbent (mg/g)
q_{exp}	Experimental equilibrium capacity (mg/g)
q_m	Maximum adsorption capacity of adsorbent (mg/g)
q_S	Khan isotherm maximum adsorption capacity (mg/g)
q_t	Adsorption capacity of adsorbent (mg/g) in t
R_L	Dimensionless constant of separation factor
r_P	Radke-Prausnitz isotherm model constant $\text{L}^{(1-b)}\text{g}^{-1}\text{mg}^b$
t	Toth isotherm model exponent
β_K	Radke-Prausnitz isotherm model exponent

REFERENCES

- B. Royer, N.F. Cardoso, E.C. Lima, J.C.P. Vaghetti, N.M. Simon, T. Calvete and R.C. Veses, *J. Hazard. Mater.*, **164**, 1213 (2009).
- T. Robinson, G. McMullan, R. Marchant and P. Nigam, *Bioresour. Technol.*, **77**, 247 (2001).
- A. Mittal, J. Mittal and L. Kurup, *J. Hazard. Mater.*, **136**, 567 (2006).
- D.S. Brookstein, *Dermatol. Clin.*, **27**, 309 (2009).
- M.A. Behnajady, N. Modirshahla, N. Daneshvar and M. Rabbani, *Chem. Eng. J.*, **127**, 167 (2007).
- V.K. Gupta and Suhas, *J. Environ. Manage.*, **90**, 2313 (2009).
- M.A. Rauf, S.B. Bukallah, A. Hamadi, A. Sulaiman and F. Hammadi, *Chem. Eng. J.*, **129**, 167 (2007).
- G. Crini, *Bioresour. Technol.*, **97**, 1061 (2006).
- P. Luo, Y. Zhao, B. Zhang, J. Liu, Y. Yang and J. Liu, *Water Res.*, **44**, 1489 (2010).
- A.K. Mishra, T. Arockiadoss and S. Ramaprabhu, *Chem. Eng. J.*, **162**, 1026 (2010).
- G.D. Sheng, D.D. Shao, X.M. Ren, X.Q. Wang, J.X. Li, Y.X. Chen and X.K. Wang, *J. Hazard. Mater.*, **178**, 505 (2010).
- V.K. Gupta, S. Agarwal and T.A. Saleh, *Water Res.*, **45**, 2207 (2011).
- N.S. Lawrence and J. Wang, *Electrochem. Commun.*, **8**, 71 (2006).
- Y.-H. Li, Z. Di, J. Ding, D. Wu, Z. Luan and Y. Zhu, *Water Res.*, **39**, 605 (2005).
- F.M. Machado, C.P. Bergmann, T.H.M. Fernandes, E.C. Lima, B. Royer, T. Calvete and S.B. Faganc, *J. Hazard. Mater.* (In press).
- S. Chatterjee, M.W. Lee and S.H. Woo, *Bioresour. Technol.*, **101**, 1800 (2010).
- C.-H. Wu, *J. Hazard. Mater.*, **144**, 93 (2007).
- P.R. Chang, P. Zheng, B. Liu, D.P. Anderson, J. Yu and X. Ma, *J. Hazard. Mater.*, **186**, 2144 (2011).
- C.-Y. Kuo, C.-H. Wu and J.-Y. Wu, *J. Colloid Interf. Sci.*, **327**, 308 (2008).
- J.-L. Gong, B. Wang, G.-M. Zeng, C.-P. Yang, C.-G. Niu, Q.-Y. Niu, W.-J. Zhou and Y. Liang, *J. Hazard. Mater.*, **164**, 1517 (2009).
- M. Zhao and P. Liu, *Micropor. Mesopor. Mater.*, **112**, 419 (2008).
- H. Yu and B. Fugetsu, *J. Hazard. Mater.*, **177**, 138 (2010).
- M. Trojanowicz, *Trends Analyt. Chem.*, **25**, 480 (2006).
- S. Iijima, *Nature*, **354**, 56 (1991).
- R.B. Rakhi, K. Sethupathi and S. Ramaprabhu, *Carbon*, **46**, 1656 (2008).
- A.L.M. Reddy and S. Ramaprabhu, *J. Phys. Chem. C*, **111**, 7727 (2007).
- N. Jha and S. Ramaprabhu, *J. Appl. Phys.*, **106**, 84317 (2009).
- S.K. Milonjic, A.L. Ruvarac and M.V. Susic, *Thermochim. Acta*, **11**, 261 (1975).
- D.J. Nelson, H. Rhoads and C. Brammer, *J. Phys. Chem. C*, **111**, 17872 (2007).
- H. Zhang, G. Lin, Z. Zhou, X. Dong and T. Chen, *Carbon*, **40**, 2429 (2002).
- I. Langmuir, *J. Am. Chem. Soc.*, **40**, 1361 (1918).

32. T.W. Weber and R.K. Chakravorti, *AIChE J.*, **20**, 228 (1974).
33. H.M.F. Freundlich, *J. Phys. Chem.*, **57**, 385 (1906).
34. F. Haghseresht and G. Lu, *Energy Fuels*, **12**, 1100 (1998).
35. M.I. Tempkin and V. Pyzhev, *Acta Phys. Chim. USSR*, **12**, 327 (1940).
36. M.M. Dubinin and L.V. Radushkevich, *Proc. Acad. Sci. USSR Phys. Chem. Sect.*, **55**, 331 (1947).
37. O. Redlich and D.L. Peterson, *J. Phys. Chem.*, **63**, 1024 (1959).
38. R. Sips, *J. Chem. Phys.*, **16**, 490 (1948).
39. J. Toth, *Acta Chem. Acad. Hung.*, **69**, 311 (1971).
40. Y.S. Ho, J.F. Porter and G. McKay, *Water Air Soil Pollut.*, **141**, 1 (2002).
41. A.R. Khan, R. Atallah and A. Al-Haddad, *J. Colloid Interf. Sci.*, **194**, 154 (1997).
42. R.A. Koble and T.E. Corrigan, *Ind. Eng. Chem.*, **44**, 383 (1952).
43. C.J. Radke and J.M. Prausnitz, *Ind. Eng. Chem. Fund.*, **11**, 445 (1972).
44. S. Rengaraj, J.-W. Yeon, Y. Kim, Y. Jung, Y.-K. Ha and W.-H. Kim, *J. Hazard. Mater.*, **143**, 469 (2007).
45. M. Kara, H. Yuzer, E. Sabah and M.S. Celik, *Water Res.*, **37**, 224 (2003).